

Article

Development of Manganese-Coated Graphite Electrode in a Dual-Chambered Fuel Cell for Selenite Removal and Bio-Electricity Generation from Wastewater Effluent by *Bacillus cereus*

Jayanthi Velayudhan and Sangeetha Subramanian * 

School of Bioscience and Technology, Vellore Institute of Technology, Vellore 632014, India

* Correspondence: sangeethasubramanian@vit.ac.in

Abstract: A manganese oxide-coated cylindrical graphite cathode with a zinc anode was developed to treat wastewater containing selenite in a dual-chambered microbial fuel cell. COD and selenite removal in the anodic chamber by *Bacillus cereus* with energy generation were evaluated in batch mode. A manganese dioxide-coated graphite cathode was tested for its surface morphology and chemical composition using scanning electron microscopy and dispersive energy analysis of X-rays. Compared to the non-coated graphite electrode, up to 69% enhancement was observed in the manganese dioxide-coated electrode voltage generation with 150 ppm selenite concentration. The fuel cell achieved a maximum power density of 1.29 W/m² with 91% selenite reduction and up to 74% COD (initial COD of 120 mg/L) removal for an initial selenite concentration from 100 to 150 ppm. The current study demonstrated the possibility of a modified cathode in enhancing energy generation and the use of microbial fuel cell technology to treat wastewater containing selenite.

Keywords: manganese dioxide; graphite cathode; microbial fuel cell; selenite; wastewater treatment; COD



Citation: Velayudhan, J.; Subramanian, S. Development of Manganese-Coated Graphite Electrode in a Dual-Chambered Fuel Cell for Selenite Removal and Bio-Electricity Generation from Wastewater Effluent by *Bacillus cereus*. *Energies* **2023**, *16*, 2880. <https://doi.org/10.3390/en16062880>

Academic Editor: Vladimir Gurau

Received: 29 November 2022

Revised: 6 February 2023

Accepted: 15 February 2023

Published: 21 March 2023



Copyright: © 2023 by the authors. Licensee MDPI, Basel, Switzerland. This article is an open access article distributed under the terms and conditions of the Creative Commons Attribution (CC BY) license (<https://creativecommons.org/licenses/by/4.0/>).

1. Introduction

Selenium (Se) is necessary for human and animal metabolism at trace levels. Various inorganic forms of selenium, such as selenide, selenate, and selenite, are found in nature. The accumulation rate of selenium in the environment increases due to industrial and agricultural operations [1]. Numerous industries, such as the glass production and electronic sectors, use selenium and its compounds extensively, and waste streams from these sectors will release significant amounts of selenium. Additionally, when agricultural run-off travels across the dry terrain, water systems might be contaminated with soluble selenium compounds (selenate and selenite), and when the water evaporates, they concentrate in wetlands. Selenium leaches from coal fly ash, mining, metal smelting, processing crude oil, and landfills, contaminating rivers and other water bodies. Wetland birds, fish, and other oviparous species were reported to develop congenital abnormalities due to high selenium levels in rivers [2]. Elevated dietary methylmercury concentrations can aggravate selenium toxicity's negative effects in oviparous animals [3]. The mining of phosphates and metal ores, sewage sludge, fly ash from coal-fired power stations, oil refineries, and agricultural drainage are also the causes of the toxic contamination of Se in the aquatic environment [1,2,4].

Microbes transform water-soluble forms of Se into insoluble elemental Se [2,5]. Compared to other Se species, elemental Se is less toxic, as well as its bioavailability. Removing Se from industrial wastewater was difficult and not cost effective due to the combination of high volume and low concentration of Se [6]. The Se from the waste stream could be removed by various technologies, such as adsorptive, physical, oxidative, or reductive biological techniques. Bioreactors can convert soluble Se to its elemental form [4,7]. High

Se removal was achieved using anaerobic granular sludge in an up-flow anaerobic sludge blanket reactor [8,9]. Domestic and industrial wastewater is subject to conventional aerobic treatment, which involves substantial capital costs as well as high operational and energy costs. Microbial fuel as an alternative technique for traditional wastewater treatment can aid in the recovery of energy from wastewater and reduce the amount of energy input and excessive sludge formation [10].

Microbial fuel cells (MFCs) may employ bacteria to oxidize organic and inorganic substrates and produce power. This approach significantly produced power from wastewater's common organic materials, such as proteins and carbohydrates, while also cleaning up harmful substances such as phenols and petroleum compounds [11]. According to the previous research studies carried out by Thiviraj Chellamuthu et al., 2011 [12] and Catal et al., 2008 [13], on the possible removal of Se using MFCs. Single-chambered MFCs were developed for the removal of selenite from wastewater treatment. However, there is still no research on the reduction of selenite from domestic wastewater and electricity production by a dual-chambered microbial fuel cell [14]. Single-chamber fuel cells are less effective compared to dual-chambered fuel cells in electricity generation. The main advantage of dual chambers over single chambers is the ability to improve performance through pH adjustment, organic load enhancement, oxygen purging, and enhancement of electron mediators in the cathode, which results in improved MFC performance. Due to a higher rate of oxygen diffusion and substrate crossing, the single-chamber structure has the disadvantage of having poor Coulombic efficiency. High power densities cannot be achieved with single MFCs because the anode and cathode must be closed. Short retention times with a single MFC might decrease the COD removal efficiency; hence, with higher volumes, the treatment is not as effective as other biological treatments since the retention times do not permit the removal of high COD concentrations [14,15].

The performance of MFC could be achieved by several means, such as the cathode material used, the pH maintained in the chamber, flow rate enhancement, oxygen purging, and the use of electron mediators in the cathode [16]. The bacteria interact with the electrode and oxidize the organic substrate and produce electrons and protons through glycolysis, the Krebs cycle, and the electron transport chain [17]. Because of the slow reaction kinetics, electron uptake in the anode [11] and cathode [14,15] is regarded as a key factor in limiting the amount of power produced by MFCs.

The cathode material of the microbial fuel cell plays an important role in capturing protons among all components in MFCs. Cathode performance has an effect on oxygen reduction kinetics [18]. Various modifications were made to the electrode material to improve electricity generation. The most common and economical electrode materials in MFCs for producing biocompatible electrodes are carbon-based (cloth, felt, and paper) and non-inert metallic materials. The hydrophobic properties of the electrode materials frequently enhance the interfacial resistance as a result of microorganisms' ineffective adherence to the electrode surface [16,17,19]. The use of quinones [18,20], Mn^{4+} [21], and neutral red [21,22] as electroactive mediator species to promote quicker electron transport is among them. Other techniques used for electrode modification include conducting polymers [20], carbon nanotubes (CNTs) [23,24], and metal particles [16,25]. According to earlier studies, coating carbonaceous electrode material with metal and metal oxides enhances the electroactive microbial population, improving the performance of fuel cells. When compared to an uncoated electrode, electrodes modified with Au [24], Pd, manganese dioxide (MnO_2), iron oxides [16,25], ruthenium oxide [26], and electrodeposition of nickel-iron (NiFe) and nickel-iron-phosphorous (NiFeP) nanostructures [27] performed better.

Various physical and chemical modifications to carbon materials have been documented in the past in order to increase conductivity, surface area, and biocompatibility for microbial growth [26]. Compared to bare (unmodified) carbon electrodes, the oxygen reduction reaction (ORR) has a large over-potential barrier, which necessitates the addition of a catalyst such as Pt [8]. Although Pt is a common ORR catalyst in MFCs [28], due to its expensive cost and activity loss from extra reactions [29–31], researchers have been

looking for non-Pt catalysts that can be utilized in place of Pt without significantly affecting MFC performance. Cobalt tetramethyl phenyl porphyrin (CoTMPP) [32,33], iron cobalt tetramethyl phenyl porphyrin (FeCoTMPP) [34], cobalt tetramethyl phenyl porphyrin (FeCoTMPP), MnO_2 [8], Fe_2O_3 [29], and activated carbon fabric (ACF) [35] have all been proven to contribute to power generation in MFCs. Manganese, a less costly catalyst than platinum, has proven to be efficient at facilitating power outputs in MFCs and catalyzing oxygen reduction reactions [24]. Because of their availability, low cost, environmental friendliness, and significant catalytic activity towards the electrochemical ORR, Mn oxides have received great interest as cathode catalysts in MFC. So, this research addressed the feasibility of using MnO_2 as a low-cost alternative cathode catalyst to platinum. According to the previous literature support, there are only a few studies focused on the development of MnO_2 -based cathode electrodes for simultaneous selenite reduction, COD removal, and bioelectricity production. Additionally, the development of dual-chambered fuel for domestic wastewater treatment with a zinc anode and MnO_2 coated cathode electrodes for fuel cells is needed.

The aim of this study was to investigate the ability of *Bacillus cereus* to produce bioelectricity and to effectively reduce the selenite in a dual-chamber MFC with an MnO_2 -coated graphite cathode. Selenite reduction conditions and bioelectricity production by *Bacillus cereus* were studied in comparison with MnO_2 coated and uncoated graphite cathodes. The capability of MFC technology to significantly remove Selenite was found, and the possibility of employing it to treat wastewaters that include Selenite was examined. This study could result in the generation of less sludge, which can be converted into biochar and used as an adsorbent, catalyst carrier, soil conditioner, and cement paste [36].

2. Material and Method

All the chemicals and media (Luria Bertani broth, agarose, potassium chloride, potassium permanganate, polyethylene glycol, sodium selenite, potassium dichromate, mercuric sulfate, sulphuric acid, ferrous ammonium sulfate, and ferroin indicator) were procured from Himedia Chemicals Limited, India. Graphite and zinc electrodes were purchased from Agilent graphite furnace AAS electrodes, Agilent Technologies India Pvt. Ltd. (Chennai). The *Bacillus cereus* was isolated from seawater in the coastal region of Mumbai, Maharashtra (Accession Number-KR611712).

2.1. Design of the Microbial Fuel Cell Setup

The experimental design of the constructed dual-chamber MFC is clearly shown in Figure 1. The MFC was designed using 2 borosilicate glass chambers with an effective volume of 1000 mL, each connected using a (proton exchange membrane) salt bridge made of 2% agarose with 10% potassium chloride (KCl) [24,25]. The proton exchange membrane acts as a semi-permeable membrane and a reactant barrier prevents the transfer of substrate, minerals, and oxygen from the anodic chamber to the cathodic chamber. The agarose and potassium chloride in the salt bridge facilitates the significant transfer of the proton to the cathode in turn increases the rate of electricity generation. The concentration of salt will increase the conductivity of the salt agar bridge system; thereby, it controls internal resistance [25]. Graphite (MnO_2 coated and uncoated) with a surface area of 0.35 square meters was used as the cathode and zinc was used as the anode (surface area of 0.35 square meters).

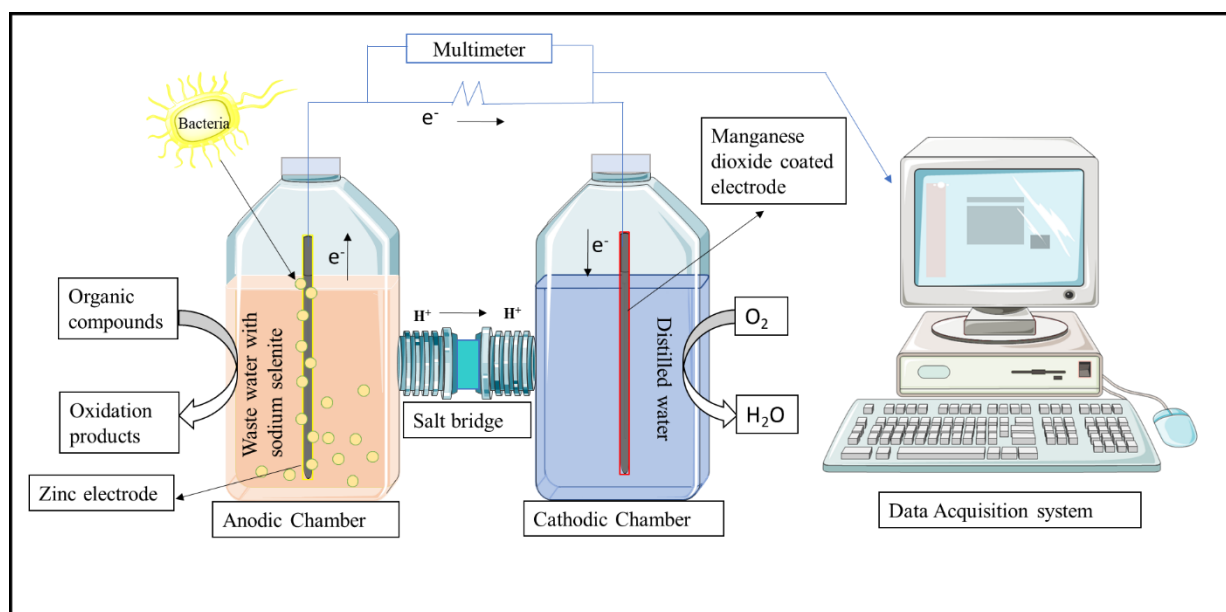


Figure 1. Experimental design of dual-chamber MFC.

Non-inert metallic electrode-based MFC was developed in recent years to obtain a better performance in the electricity generation. According to earlier research, oxidation always takes place at the anode and involves electron loss. Due to the oxidation of Zn atoms on the electrode give up two electrons and become Zn^{2+} when they enter the solution ($Zn^{2+}(aq)/Zn(s)$ half-cell). Electrons always go from the anode to the cathode in a voltaic cell. The common carbon electrodes are replaced with the metal electrode in the anodic chamber [19]. For example, the Zinc electrode was used as an anode since it has good reduction potential ($Zn^{2+} + 2e \rightarrow Zn$ ($E^{\circ} = -0.763 V$)) [20,26]. Zinc (amphoteric metal) can react with both acid and alkali. It has the potency to work in all ambient conditions in the microbial fuel cell. In 2015, Das used zinc mesh as an anode electrode in algal MFC and he achieved good performance compared to the use of other carbon derived electrodes. Additionally, in 2016, Cek reported in his work that moss MFC used a Zn anode electrode and obtained good performance [18,26]. Due to all these properties, the zinc electrode was used as an anode in this study.

The MFC with the zinc anode and the graphite cathode, along with LB broth (anolyte) and distilled water (catholyte), serves as the control. With the help of LabVIEW (2015), the voltage output and the potential of the cathode and/or anode were measured. The voltage was recorded through a data acquisition unit (DAQ USB-6221, National Instruments Co., Ltd., Guangdong, China) [6,37]. There was no additional oxygen supply provided to the system, and the cathodic chamber was left open to absorb oxygen from the atmosphere.

2.2. Preparation of Cathodic Material

The deposition of MnO_2 crystals onto the cylindrical graphite electrode was carried out by immersion technique. Initially, 4.16 g of potassium permanganate was dissolved in 500 mL of double-distilled water and stirred continuously to facilitate uniform mixing. The electrode was immersed in this solution, and 45.83 g of polyethylene glycol (reducing agent) was added slowly. Then, the flask was stirred for 90 min. The redox reactions between potassium permanganate and polyethylene glycol (PEG) resulted in the formation of a brown color precipitate and was observed on the electrode. The electrode was then dried at 100 °C for 90–120 min [24,25].

2.3. Preparation of Anodic and Cathodic Chamber

The constructed laboratory-scale MFC was operated in batch mode with secondary treated wastewater spiked with different concentrations of selenite (100 and 150 ppm). Secondary treated domestic wastewater was collected from the sewage treatment plant of the Vellore Institute of Technology, Vellore, Tamil Nadu, India, and the chemical composition is shown in Table 1. The distilled water was used as a catholyte in the cathodic chamber. The analyte for the anodic chamber was prepared with an equal volume of the above-mentioned wastewater and the Luria Bertani broth containing yeast extract, NaCl, and tryptone as an added nutrient and spiked with varying concentrations of sodium selenite (100 and 150 ppm) [6,16]. The collected wastewater was initially characterized by the Tamil Nadu pollution control board in Gandhi Nagar, Vellore (Table 1).

Table 1. Chemical components of the wastewater.

Content	Values and Units
pH	6.8
Suspended solids	100 to 150 mg/L
Total dissolved solids	16 mg/L
BOD	100–180 mg/L
COD	250 mg/L
Oil and grease	10–100 mg/L

An actively growing *Bacillus cereus* was grown in LB broth for 12–15 h in a shake flask at 121 rpm in an orbital shake. Then the culture was centrifuged, and the pellet was used as inoculum to start the experiment. The MFC was operated at pH 6.8 and at room temperature for 72 hrs. The samples were analyzed for COD and selenite removal after 24, 48, and 72 h [27,28,37]. The bacteria in the anodic chamber act on the biodegradable organic matter to release protons and electrons. The electrons are transported to the cathodic chamber via the external circuit, and the protons, on the other hand, are transported through the proton exchange membrane. This flow of ions generates electricity in the microbial fuel cell.

2.4. Electrochemical Measurement and Analysis

The voltage generated in the microbial fuel cell was recorded regularly using a data acquisition system. The circuit current was calculated using Ohm's law ($V = IR$). The current and power density values were assessed by the formula given below:

$$\text{Voltage} = IR \quad (1)$$

$$\text{Power} = \frac{V^2}{R} \quad (2)$$

$$\text{Power density} = \frac{\text{Power}}{\text{Surface area of electrode}} \quad (3)$$

$$\text{Volumetric power} = \frac{\text{Power}}{\text{Volume (1000 mL)}} \quad (4)$$

where

I —Current in Ampere

R —Resistance

V^2 —A voltage applied across the two ends

The COD of the samples at 24, 48, and 72 h were determined using potassium dichromate as the reducing agent and titrated against ferrous ammonium sulfate. The COD removal was measured using the given formula:

$$\text{COD} = \frac{8 \times 1000 \times D.F \times M \times (V_B - V_S)}{V_{\text{Sample}}} \quad (5)$$

$D.F$ —Dilution Factor

M —Molarity of Ferrous ammonium sulphate

V_B —Volume of Ferrous ammonium sulphate used by blank (mL)

V_S —Volume of Ferrous ammonium sulphate used by Sample at time, t (mL)

$$\text{COD Removal percentage} = \frac{\text{COD}_{\text{in}} - \text{COD}_{\text{out}}}{\text{COD}_{\text{in}}} \times 100 \quad (6)$$

COD_{in} —Initial concentration of COD (g L^{-1})

COD_{out} —Final concentration of COD at time, t (g L^{-1})

By integrating the current (I) observed over time (t) and comparing it with the theoretical current based on the change in chemical oxygen demand (COD) removed from the following equation, Coulombic efficiency (CE) was determined:

$$\text{CE} = \frac{8 \int_0^t I d(t)}{F V_{\text{anode}} \Delta\text{COD}} \quad (7)$$

where 8 is a constant used for COD, based on MO_2 32 g mol^{-1} , 4 electrons exchanged per mole of oxygen, F is the Faraday's constant ($96,485 \text{ C mol}^{-1}$ -electrons), V_{anode} is the volume of the anode chamber, and ΔCOD is the change the COD over time (t) [29].

The bacteria in the anodic chamber reduced the soluble selenite to insoluble selenium, and the red precipitate forms and the soluble selenite were measured using the ICP-AES (SPECTRO Analytical Instruments, ARCOS, Simultaneous ICP Spectrometer). The samples were withdrawn after 24, 48, and 72 h and centrifuged at 8000 rpm for 15 min. The supernatant was collected and filtered with a $0.45 \mu\text{m}$ syringe filter, and the selenite concentration was measured. The given formula measured the selenite removal percentage as follows:

$$\% \text{ Selenite removal} = \frac{A - B}{A} \times 100 \quad (8)$$

A —Initial soluble selenite concentration

B —Soluble selenite concentration at time, t

2.5. Morphological Analysis

The MnO_2 graphite electrode was investigated using the SEM imaging technique with a magnification of $7000\times$ at $2 \mu\text{m}$, EHT of 10 kV, and a WD of 11 mm. The images of coated and uncoated electrodes were compared to study the presence of coating and its uniform distribution. Energy dispersive X-ray (EDAX) analysis was performed to confirm the chemical composition of the electrode.

3. Results and Discussion

3.1. Morphological Characterization of Manganese Dioxide (MnO_2) Electrode

The cathode of the microbial fuel cell plays a crucial role in proton capture among all components in MFCs. The graphite cathode was coated with MnO_2 to improve proton capture and electricity production. The scanning electron microscopy (SEM) technique was used to study the surface and morphological characteristics of the MnO_2 -coated and uncoated graphite cathodes. The electrode was cut into 1 cm size for SEM analysis. Figure 2A shows the outer surface of the electrode, and Figure 2B shows the surface characteristics of the graphite cathode coated with MnO_2 used in MFC. Figure 2B showed the presence

of a uniform distribution of small manganese particles, an additional layer on the coated electrode that was absent on the uncoated electrode. To confirm the chemical composition of the MnO_2 layer, an EDAX analysis was performed. The absence of manganese particles was observed on the uncoated electrode. The primary component, carbon, constitutes 85% of the total composition and 10% oxygen in the uncoated electrode. On the other hand, the coated electrode had 30% carbon, 23% manganese, and 27% oxygen, confirming the presence of a MnO_2 layer on the surface of the electrode (Figure 2B) [24].

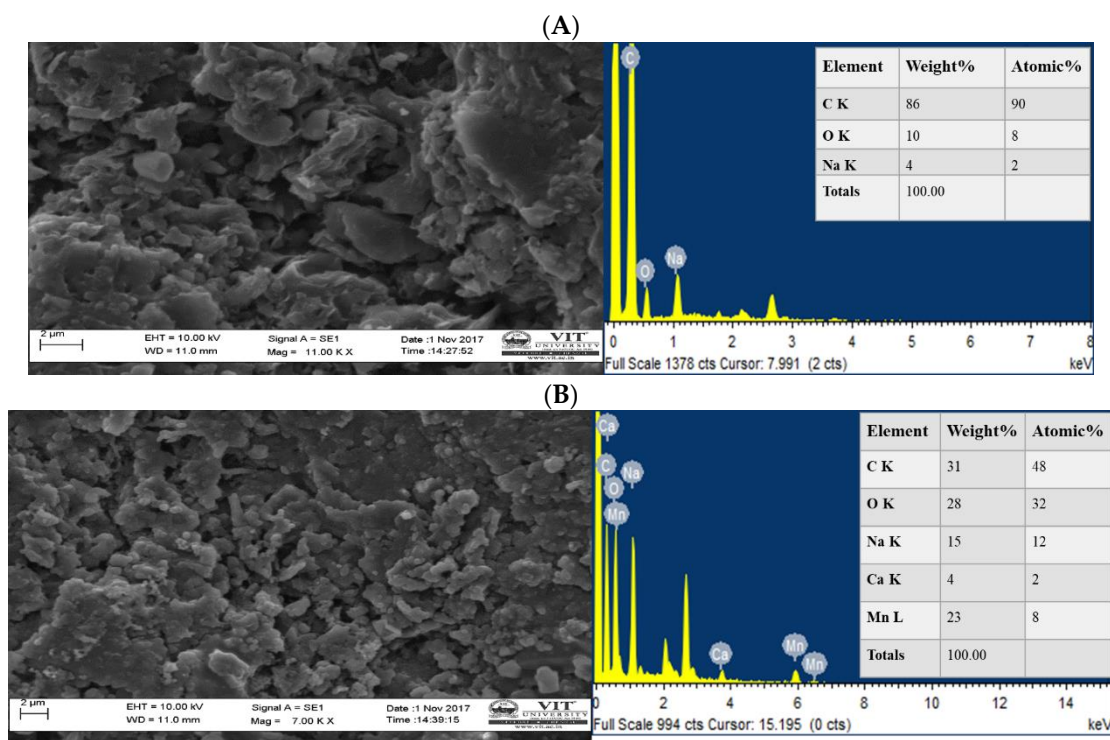


Figure 2. SEM image of (A) graphite electrode and (B) graphite electrode coated with manganese dioxide.

3.2. Effect of Selenite Concentration on Bioelectricity Generation

The laboratory-scale microbial fuel cell was constructed with *Bacillus cereus* to treat secondary treated wastewater containing varying concentrations of selenite (100 and 150 ppm) at neutral pH [5]. Parameters such as pH, substrate concentration, and the biological organic matter of the wastewater residue will affect MFC's electricity generation. A set of controls were performed to validate the microbe's contribution to energy production. The MFC with a zinc anode and graphite cathode (MnO_2 coated and uncoated) with the Luria Bertani broth containing selenite (100 and 150 ppm) without wastewater (control) was also studied and compared with wastewater containing selenite (100 and 150 ppm) for energy production. It was evident from Table 2 and Figure 3 that there was higher voltage production in the presence of wastewater with a higher concentration of selenite than in the control run. Overall, there was a 16.3% increase in the voltage of the MFC setup with the uncoated graphite electrode and a 31% increase with the coated graphite electrode.

Table 2. Other reported surface modified cathode material on microbial fuel cell.

S No.	Cathode Material	Type of Cathode	Power Density (Wm^{-2})	Reference
1.	NaCo ₂ O ₄ carbon cathode	Air-cathode	0.6	[38]
2.	Manganese dioxide/titanium dioxide/graphitic carbon nitride coated granular activated carbon cathode	-	1.17	[39]
3.	MnO ₂ nanotubes/graphene oxide nanocomposite modified cathode	Air-breathing cathode	3.359	[40]
4.	Fe-Ag-N multi-doped graphene Cathode	Air-cathode	1.96	[41]
5.	α -MnO ₂ Nanosheet	Air-cathode	1.671	[42]
6.	Graphene oxide-supported zinc cobalt oxide cathode	-	0.773	[43]
7.	MnO ₂ @rGO Cathode	-	0.008	[44]
8.	BGQDs/MOF-15 cathode	-	0.703	[45]
9.	Manganese dioxide coated graphite cathode	-	1.29 W/m ²	This study

In the MFC operation, Dhiraj et al. [35] reported using a graphite electrode and a PbO₂ graphite electrode with river water as the electrolyte; a maximum voltage of 937 mV, a maximum current density of 382 A cm⁻², and a maximum power density of 86 W cm⁻² were achieved. Additionally, Venkatamohan et al. [32] obtained a maximum current density of 62.23 mA m⁻² and a maximum power density of 15.56 mW m⁻² using the hybrid electrode with Musi River water as the electrolyte. A near-neutral pH was said to be advantageous for electricity generation and COD elimination. In contrast, operational pH values greater than 10 have been observed to be less suited for collecting bioelectricity [33]. As a result, the pH was kept neutral throughout the investigation.

There was an increase in the current production in the fuel cell setup with MnO₂-coated graphite cathode because of the pseudo-capacitive character of the MnO₂. According to Ma et al., 2008, MnO₂ in an aqueous neutral electrolyte follows the redox reaction ($MnO_2 + \delta X^+ + \delta e^- \leftrightarrow MnOOX_\delta$) where X⁺ stands for the H⁺. The hypothetical specific capacitance of the conversion of Mn (IV)O₂ to Mn (III)OOX leads to an increase in voltage production. The continual rise in current during cyclic voltammetry charging of the electrodes may also be attributed to the creation of free protonic or cationic species (X⁺), which improve the ionic conductivity of the electrolyte [21,22]. The surface modification of a cathode with a catalyst will improve power generation. Some of the examples of the power production improvement by surface coating of cathode materials are listed in Table 2.

The redox reaction of the MnO₂ coating on the surface of the graphite electrode may be the cause of this current rise. Table 3 supports the hypothesis that coating the electrode with the conductive MnO₂ particles caused an increase in the voltage and power density obtained by the cell. In the control setup with 100 ppm of selenite and without wastewater, there was a 19.6% increase in power production compared to the uncoated cathode. However, the control with 150 ppm of selenite resulted in a 21% selenite reduction. In the experimental setup, there was a 43% and 27% increase in the voltage recorded for an initial concentration of 100 ppm and 150 ppm selenite, respectively. The power density of the setup with the coated electrode increased by 46% for an initial concentration of 100 ppm and by 69% for an initial concentration of 150 ppm. This proves the additive effect that coating has on the functioning of the microbial fuel cell. A maximum voltage of 1.22 V and 1.29 V was recorded for initial concentrations of 100 ppm/L selenite and 150 ppm, respectively.

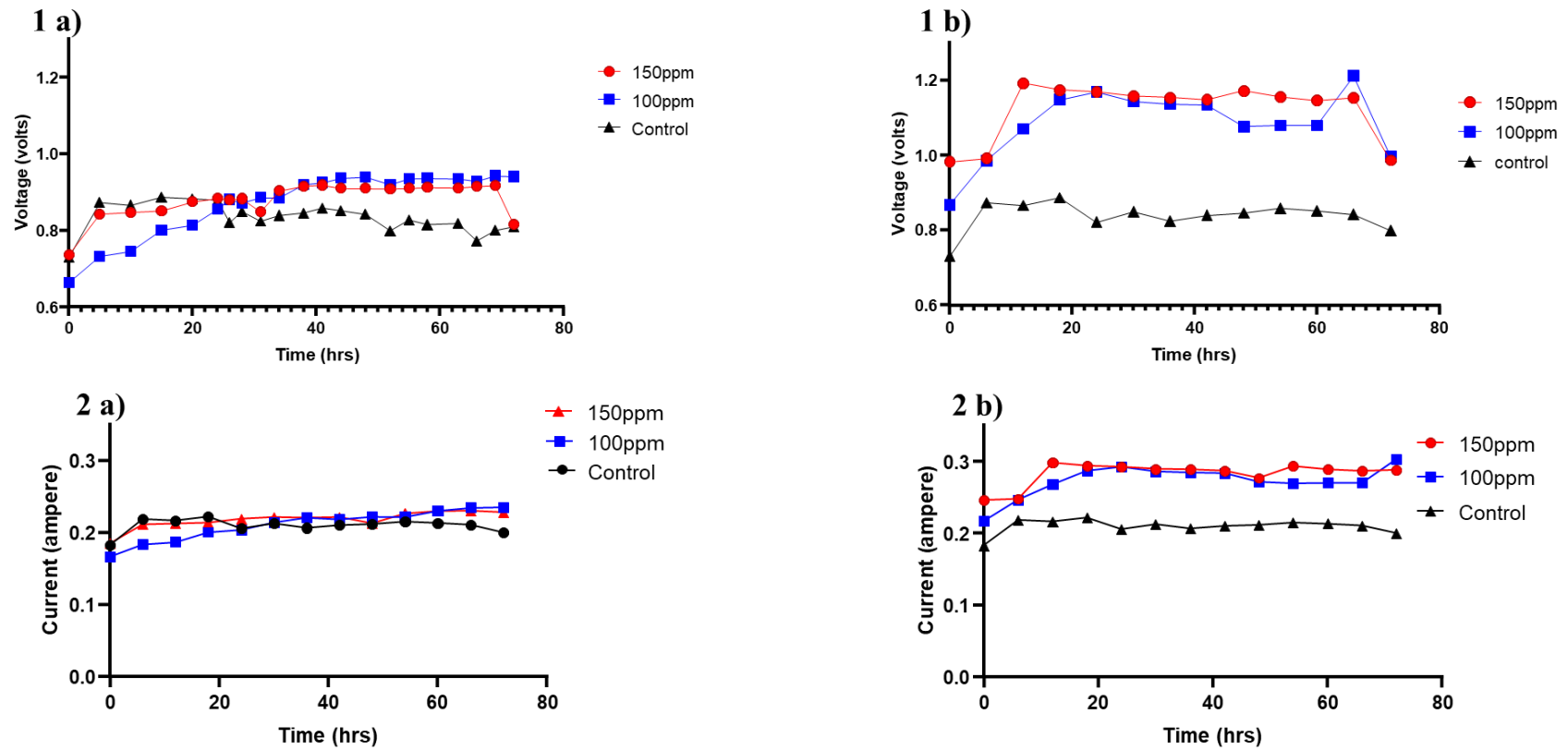


Figure 3. Cont.

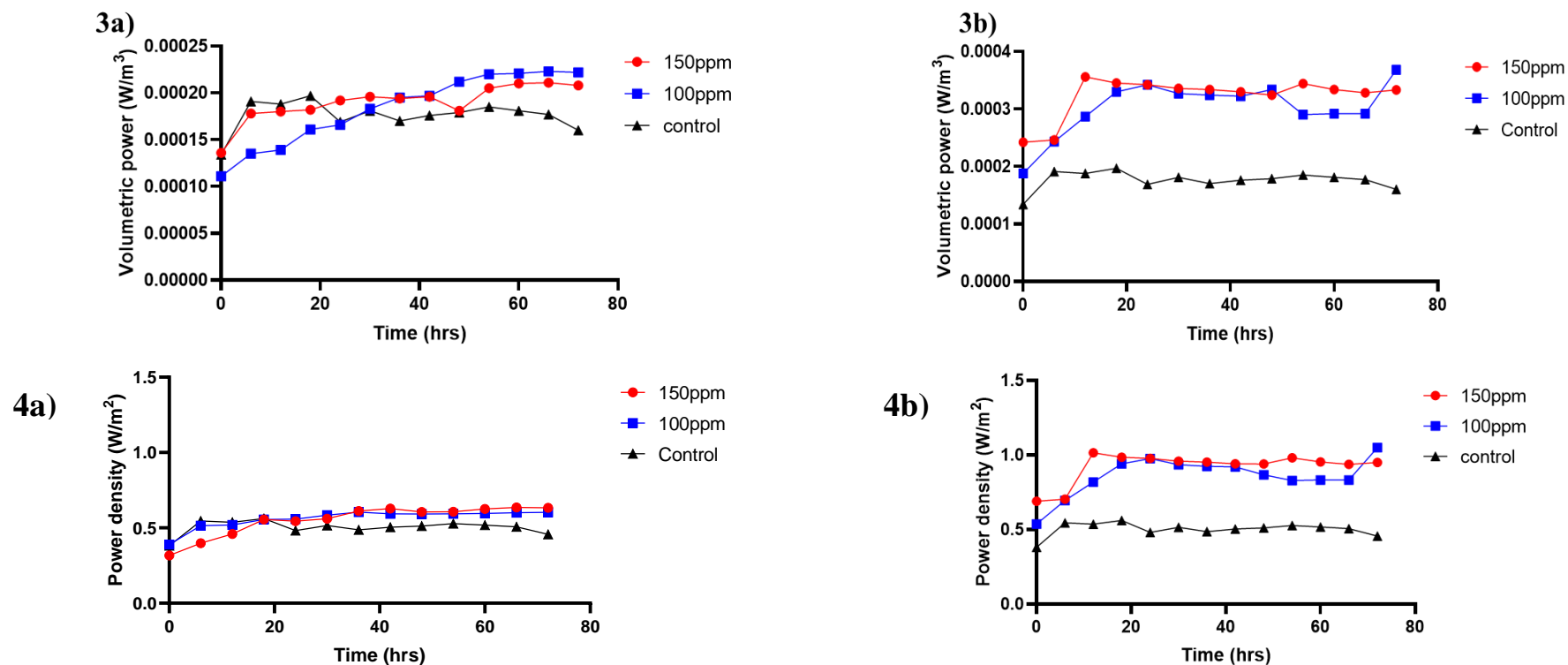


Figure 3. Time vs. voltage, current, volumetric power, and power density curves of coated (1a–4a) and uncoated manganese cathode electrodes (1b–4b). (1a) Time vs. voltage curve for an uncoated manganese cathode electrode; (1b) time vs. voltage curve for a coated manganese cathode electrode; (2a) time vs. current curve for an uncoated manganese cathode electrode; (2b) time vs. current curve for a coated manganese cathode electrode; (3a) time vs. volumetric power curve for an uncoated manganese cathode electrode; (3b) time vs. volumetric power curve for a coated manganese cathode electrode; (4a) time vs. power density for an uncoated manganese cathode electrode; and (4b) time vs. power density for a coated manganese cathode electrode.

Table 3. Voltage and power densities obtained in the control setup and MFC with varying selenite concentration.

S. No	Operating Conditions	Coating on Electrode	Maximum Voltage (V)	Maximum Power Density (W/m ²)	% Difference in Voltage Production Compared to Coated and Uncoated	% Difference in Power Density Compared to Coated and Uncoated
1	Without wastewater-100 ppm (Control)	Uncoated	0.874	0.55	-	-
2	Without wastewater-100 ppm (Control)	Coated	1.070	0.82	19.6	27
3	Without wastewater-150 ppm (Control)	Uncoated	0.67	0.32	-	-
4	Without wastewater-150 ppm (Control)	Coated	0.88	0.56	21	24
5	With wastewater-100 ppm	Uncoated	0.95	0.64	-	-
6	With wastewater-100 ppm	Coated	1.22	1.1	27	46
7	With wastewater-150 ppm	Uncoated	0.92	0.60	-	-
8	With wastewater-150 ppm	Coated	1.35	1.29	43	69

3.3. Selenite and Chemical Oxygen Demand Removal Efficiency

The COD and selenite reduction were studied to understand the treatment efficiency and energy production. The effective removal of selenite by bacteria requires carbon, energy, and electron donors. The energy harvested through the oxidation of organic waste (wastewater) at the anode of MFCs drives the reduction of selenite in the anodic chamber. Thus, the reduction and removal rates depend on the anodic chamber's bacterial and organic load [46]. In the MFC setup, there was a 91% reduction of selenite for an initial concentration of 100 ppm/L within 48–72 h and a 93% reduction for an initial concentration of 150 ppm (Figure 4). A significant reduction in the chemical oxygen demand was observed, i.e., a 74% reduction for 100 ppm/L and a 73% reduction for 150 ppm selenite concentration (Figure 4). Table 4 shows the selenite and COD removal at various operation conditions. With the rise in selenite concentration, a red deposit was seen on the MFC electrodes and in the solution. According to Narasingarao and Haggblom (2007) [47], the sediment is most likely composed of elemental selenium, produced when microorganisms in the solution and on the electrode surface reduce selenite. Tunc Catal et al., 2009, developed single-chambered fuel with mixed culture to simultaneously remove selenite and COD. In the presence of 75 ppm of selenite, 99% removal was reported in less than 48 h with 0.41 V power production with acetate as substrate and 0.07 V at 100 ppm of selenite in less than 72 h when glucose was used as substrate [16].

According to Lee et al., 2007 [30], facultative anaerobic *Shewanella* species, well known for their ability to produce electricity in MFCs, were able to use selenite as the only electron acceptor for respiration in anaerobic conditions. This resulted in selenite reduction and the precipitation of elemental Se nano-sized spherical particles. Sukkasem et al., 2008 [31], studied that denitrifying bacteria could also reduce selenite or selenate to elemental selenium, which might be crucial for electron transfer in MFCs [48]. Bacteria using organic substrates primarily for their growth and not for the creation of electrons may have contributed to the Coulombic efficiency (CE) value decreasing at high COD concentrations. Table 5 for the current study shows that the higher the organic pollutant, the lower the CE. The cathode kinetics, which were greatly enhanced by coating the cathode with MnO₂, were responsible for the maximum power output [49].

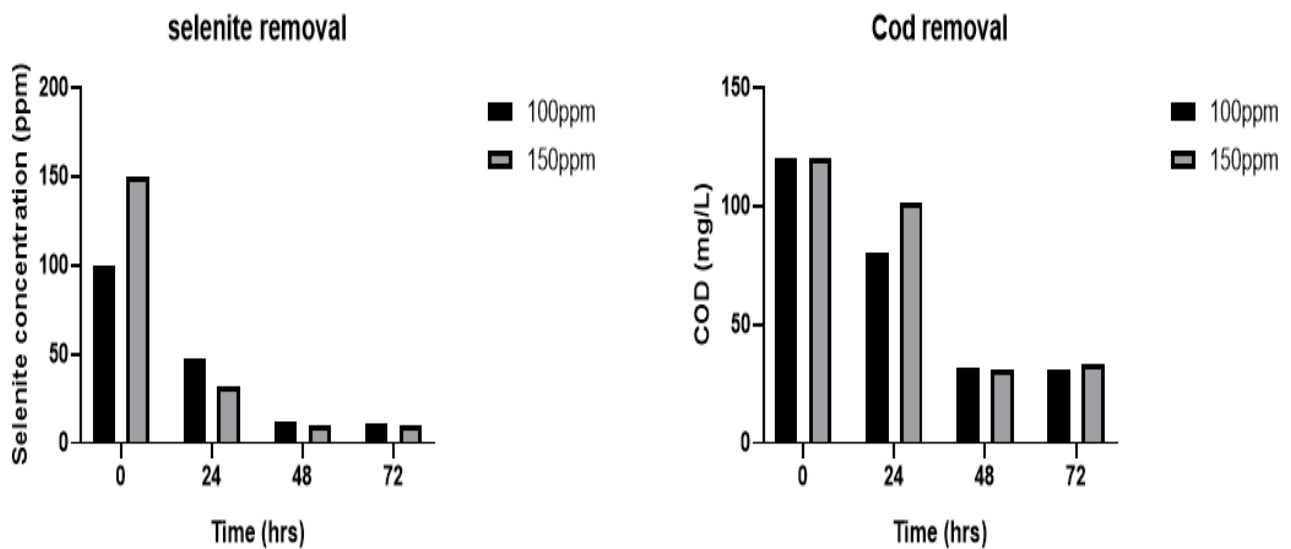


Figure 4. Percentage selenite and COD removal at 100 and 150 ppm.

Table 4. Selenite and COD removal after 72 h at varying operation conditions.

Operating Condition	Initial Selenite Concentration (ppm)	Final Selenite Concentration (ppm)	% Selenite Removal	Initial COD (mg/L)	Final COD (mg/L)	% COD Removal
Without wastewater (Control)	100	14	86	-	-	-
Without wastewater (Control)	150	9	91	-	-	-
With wastewater and selenite	100	9	91	120	31	74
With wastewater and selenite	150	7	93	120	33	73

Table 5. Removal of organics and substrate consumption in terms of Coulombic efficiency.

Time (h)	Final COD (mg/L) for Coated Electrode with 100 ppm of Selenite	Coulombic Efficiency Coated Electrode with 100 ppm of Selenite (%)	Final COD (mg/L) for Coated Electrode with 150 ppm of Selenite	Coulombic Efficiency Coated Electrode with 150 ppm of Selenite (%)
24	80	49.29	101	20.7
48	32	44.61	31	59.16
72	31	64.71	33	70.4

This finding shows that the bacteria enriched for electricity generation in the dual chamber MFC system can also use selenite as an electron acceptor [47]. As mentioned earlier, the wastewater stream polluted with Se will have different concentrations and loads. Therefore, a further enrichment step was required when the influence of MFC shifted between selenite-free and selenite-rich waste streams. These electrogens (bacteria) allow for the simultaneous generation of energy and the elimination of COD/Se, demonstrating

the enormous potential of MFC technology for wastewater treatment [16]. Residual sludge management is a critical issue since the produced sludge requires dewatering. After dewatering, the sludge was converted into biochar with selenium and used as an adsorbent for the removal of heavy metals in the wastewater (chromium, cadmium, lead, and arsenic), a catalyst carrier (MFC), and a soil conditioner (maintenance of soil pH) [36].

4. Conclusions

The research demonstrated using a MnO₂-coated graphite cathode in MFC with zinc as the anode for producing bioelectricity. MnO₂-coated graphite cathode MFC cells with a high selenite concentration exhibited enhanced energy production. Additionally, *Bacillus cereus* exhibited the reduction property by converting selenite to elemental selenium, thus playing an important role in electron transfer in MFCs. The developed technology also displayed potential for wastewater treatment by producing energy while removing COD/Se. The effect of energy generation with the variation of catholyte media, temperature, and pH, and the impact of zinc electrode erosion and biofilm formation on electrode surface, could be discussed in future studies.

Author Contributions: Conceptualization, S.S.; Investigation, J.V.; Writing—original draft, J.V.; Project administration, S.S. All authors have read and agreed to the published version of the manuscript.

Funding: This research received no external funding.

Data Availability Statement: The data presented in this study are available in article.

Conflicts of Interest: The authors declare no conflict of interest.

References

1. Hamilton, S. Review of selenium toxicity in the aquatic food chain. *Sci. Total Environ.* **2004**, *326*, 1–31. [[CrossRef](#)] [[PubMed](#)]
2. Tan, L.C.; Nancharaiyah, Y.V.; Van Hullebusch, E.D.; Lens, P.N.L. Selenium: Environmental significance, pollution, and biological treatment technologies. *Biotechnol. Adv.* **2016**, *34*, 886–907. [[CrossRef](#)]
3. Rovira, M.; Giménez, J.; Martínez, M.; Martínez-Lladó, X.; De Pablo, J.; Martí, V.; Duro, L. Sorption of selenium(IV) and selenium(VI) onto natural iron oxides: Goethite and hematite. *J. Hazard. Mater.* **2008**, *150*, 279–284. [[CrossRef](#)] [[PubMed](#)]
4. Lemly, A.D. Ecosystem Recovery Following Selenium Contamination in a Freshwater Reservoir. *Ecotoxicol. Environ. Saf.* **1997**, *36*, 275–281. [[CrossRef](#)] [[PubMed](#)]
5. Fujita, M.; Ike, M.; Kashiwa, M.; Hashimoto, R.; Soda, S. Laboratory-scale continuous reactor for soluble selenium removal using selenate-reducing bacterium, *Bacillus* sp. SF-1. *Biotechnol. Bioeng.* **2002**, *80*, 755–761. [[CrossRef](#)] [[PubMed](#)]
6. Yang, L.; Wu, Z.; Wu, J.; Zhang, Y.; Li, M.; Lin, Z.Q.; Bañuelos, G. Simultaneous removal of selenite and electricity production from Se-laden wastewater by constructed wetland coupled with microbial fuel cells. *Selenium Environ. Hum. Health* **2014**, *212*, 212–214. [[CrossRef](#)]
7. Holmes, A.B.; Gu, F.X. Emerging nanomaterials for the application of selenium removal for wastewater treatment. *Environ. Sci. Nano* **2016**, *3*, 982–996. [[CrossRef](#)]
8. Astratinei, V.; Van Hullebusch, E.; Lens, P. Bioconversion of Selenate in Methanogenic Anaerobic Granular Sludge. *J. Environ. Qual.* **2006**, *35*, 1873–1883. [[CrossRef](#)]
9. Adeniran, J.A.; Huberts, R.; De-Koker, J.J.; Arotiba, O.A.; Olorundare, O.F.; Van-Zyl, E.; Du-Plessis, S.C. Energy generation from domestic wastewater using sandwich dual-chamber microbial fuel cell with mesh current collector cathode. *Int. J. Environ. Sci. Technol.* **2016**, *13*, 2209–2218. [[CrossRef](#)]
10. Aelterman, P.; Rabaey, K.; Clauwaert, P.; Verstraete, W. Microbial fuel cells for wastewater treatment. *Water Sci. Technol.* **2006**, *54*, 9–15. [[CrossRef](#)]
11. Reddy, T.V.; Kavya, C.; Krishna Prasad Reddy, K.; Srinivas Naik, K.; Burgula, S. Dual Chambered Microbial Fuel Cell For Bioelectricity Generation From Environmental Samples. *Int. J. Sci. Res. Publ.* **2019**, *9*, p8996. [[CrossRef](#)]
12. Chellamuthu, T.; Ward, M.; Neelson, K. Removal of Selenite with Microbial Fuel Cells Utilizing *Shewanella Oneidensis* MR-1. In Proceedings of the 2011 AIChE Annual Meeting, Minneapolis, MN, USA, 16–21 October 2011.
13. Catal, T.; Liu, H.; Bermek, H. Selenium induces manganese-dependent peroxidase production by the white-rot fungus *bjerkandera adusta* (Willdenow) P. Karsten. *Biol. Trace Elem. Res.* **2008**, *123*, 211–217. [[CrossRef](#)] [[PubMed](#)]
14. Kusmayadi, A.; Leong, Y.K.; Yen, H.W.; Huang, C.Y.; Dong, C.D.; Chang, J.S. Microalgae-microbial fuel cell (mMFC): An integrated process for electricity generation, wastewater treatment, CO₂ sequestration and biomass production. *Int. J. Energy Res.* **2020**, *44*, 9254–9265. [[CrossRef](#)]
15. Munoz-Cupa, C.; Hu, Y.; Xu, C.; Bassi, A. An overview of microbial fuel cell usage in wastewater treatment, resource recovery and energy production. *Sci. Total Environ.* **2021**, *754*, 142429. [[CrossRef](#)]

16. Catal, T.; Bermek, H.; Liu, H. Removal of selenite from wastewater using microbial fuel cells. *Biotechnol. Lett.* **2009**, *31*, 1211–1216. [[CrossRef](#)] [[PubMed](#)]
17. Jaiswal, K.K.; Kumar, V.; Vlaskin, M.S.; Sharma, N.; Rautela, I.; Nanda, M.; Arora, N.; Singh, A.; Chauhan, P.K. Microalgae fuel cell for wastewater treatment: Recent advances and challenges. *J. Water Process Eng.* **2020**, *38*, 101549. [[CrossRef](#)]
18. Liu, C.H.; Lee, S.K.; Ou, I.C.; Tsai, K.J.; Lee, Y.; Chu, Y.H.; Liao, Y.T.; Liu, C. Te Essential factors that affect bioelectricity generation by *Rhodospseudomonas palustris* strain PS3 in paddy soil microbial fuel cells. *Int. J. Energy Res.* **2021**, *45*, 2231–2244. [[CrossRef](#)]
19. Suslick, K.S. *Kirk-Othmer Encyclopedia of Chemical Technology*; John Wiley & Sons: New York, NY, USA, 1998; Volume 26, pp. 517–541.
20. Madan, G.S. *Chands Success Guide (Q&A) Inorganic Chemistry*; S. Chand Publishing: New Delhi, India, 2005; ISBN 8-12-191857-X.
21. Anwer, A.H.; Khan, M.D.; Khan, N.; Nizami, A.S.; Rehan, M.; Khan, M.Z. Development of novel MnO₂ coated carbon felt cathode for microbial electroreduction of CO₂ to biofuels. *J. Environ. Manag.* **2019**, *249*, 109376. [[CrossRef](#)]
22. Zhang, L.; Liu, C.; Zhuang, L.; Li, W.; Zhou, S.; Zhang, J. Manganese dioxide as an alternative cathodic catalyst to platinum in microbial fuel cells. *Biosens. Bioelectron.* **2009**, *24*, 2825–2829. [[CrossRef](#)]
23. Sevda, S.; Sreerishnan, T.R. Effect of salt concentration and mediators in salt bridge microbial fuel cell for electricity generation from synthetic wastewater. *J. Environ. Sci. Health* **2012**, *47*, 878–886. [[CrossRef](#)]
24. Gnana Sundara Raj, B.; Asiri, A.M.; Qusti, A.H.; Wu, J.J.; Anandan, S. Sonochemically synthesized MnO₂ nanoparticles as electrode material for supercapacitors. *Ultrason. Sonochem.* **2014**, *21*, 1933–1938. [[CrossRef](#)]
25. Wang, L.; Asheim, K.; Vullum, P.E.; Svensson, A.M.; Vullum-Bruer, F. Sponge-like porous manganese(II,III) oxide as a highly efficient cathode material for rechargeable magnesium ion batteries. *Chem. Mater.* **2016**, *28*, 6459–6470. [[CrossRef](#)]
26. Çek, N. Examination of Zinc Electrode Performance in Microbial Fuel Cells. *Gazi Univ. J. Sci.* **2017**, *30*, 395–402.
27. Abourached, C. Microbial Fuel Cell for Wastewater Treatment: Heavy Metal Removal, Sewage Sludge Treatment, and its Potential Application in Wastewater Reuse in Irrigation. Ph.D. Thesis, Oregon State University, Corvallis, OR, USA, 2014.
28. Chaijak, P.; Lertworapreecha, M.; Changkit, N.; Sola, P. Electricity generation from hospital wastewater in microbial fuel cell using radiation tolerant bacteria. *Biointerface Res. Appl. Chem.* **2022**, *12*, 5601–5609. [[CrossRef](#)]
29. Verma, M.; Mishra, V. Bioelectricity Generation by Microbial Degradation of Banana Peel Waste Biomass in a Dual-Chamber S. *Cerevisiae*-Based Microbial Fuel Cell. *SSRN Electron. J.* **2022**, *168*, 106677. [[CrossRef](#)]
30. Lee, J.-H.; Han, J.; Choi, H.; Hur, H.-G. Effects of temperature and dissolved oxygen on Se (IV) removal and Se (0) precipitation by *Shewanella* sp. HN-41. *Chemosphere* **2007**, *68*, 1898–1905. [[CrossRef](#)] [[PubMed](#)]
31. Sukkasem, C.; Xu, S.; Park, S.; Boonsawang, P.; Liu, H. Effect of nitrate on the performance of single chamber air cathode microbial fuel cells. *Water Res.* **2008**, *42*, 4743–4750. [[CrossRef](#)] [[PubMed](#)]
32. Mohan, S.V.; Saravanan, R.; Raghavulu, S.V.; Mohanakrishna, G.; Sarma, P.N. Bioelectricity production from wastewater treatment in dual chambered microbial fuel cell (MFC) using selectively enriched mixed microflora: Effect of catholyte. *Bioresour. Technol.* **2008**, *99*, 596–603. [[CrossRef](#)] [[PubMed](#)]
33. Halim, M.A.; Rahman, M.O.; Ibrahim, M.; Kundu, R.; Biswas, B.K. Effect of Anolyte pH on the Performance of a Dual-Chambered Microbial Fuel Cell Operated with Different Biomass Feed. *J. Chem.* **2021**, *2021*, 5465680. [[CrossRef](#)]
34. Halim, A. Study of the Effect of pH on the Performance of Microbial Fuel Cell for Generation of Bioelectricity. *Res. Sq.* **2021**. [[CrossRef](#)]
35. Chaudhari, D.; Dubey, H.; Kshirsagar, D.; Jadhav, V. Influence of microbial fuel cell with porous anode on voltage generation, chemical oxygen demand, chloride content and total dissolved solids. *Water Sci. Technol.* **2020**, *82*, 1285–1295. [[CrossRef](#)] [[PubMed](#)]
36. Liu, Z.; Singer, S.; Tong, Y.; Kimbell, L.; Anderson, E.; Hughes, M.; Zitomer, D.; McNamara, P. Characteristics and applications of biochars derived from wastewater solids. *Renew. Sustain. Energy Rev.* **2018**, *90*, 650–664. [[CrossRef](#)]
37. Dinh, K.L.; Wang, C.T.; Dai, H.N.; Tran, V.M.; Le, M.L.P.; Saladaga, I.A.; Lin, Y.A. Lactate and acetate applied in dual-chamber microbial fuel cells with domestic wastewater. *Int. J. Energy Res.* **2021**, *45*, 10655–10666. [[CrossRef](#)]
38. Hirooka, K.; Ichihashi, O.; Takeguchi, T. Sodium cobalt oxide as a non-platinum cathode catalyst for microbial fuel cells. *Sustain. Environ. Res.* **2018**, *28*, 322–325. [[CrossRef](#)]
39. Zhang, Q.; Liu, L. A microbial fuel cell system with manganese dioxide/titanium dioxide/graphitic carbon nitride coated granular activated carbon cathode successfully treated organic acids industrial wastewater with residual nitric acid. *Bioresour. Technol.* **2020**, *304*, 122992. [[CrossRef](#)] [[PubMed](#)]
40. Gnana kumar, G.; Awan, Z.; Suk Nahm, K.; Stanley Xavier, J. Nanotubular MnO₂/graphene oxide composites for the application of open air-breathing cathode microbial fuel cells. *Biosens. Bioelectron.* **2014**, *53*, 528–534. [[CrossRef](#)] [[PubMed](#)]
41. Lv, C.; Liang, B.; Zhong, M.; Li, K.; Qi, Y. Activated carbon-supported multi-doped graphene as high-efficient catalyst to modify air cathode in microbial fuel cells. *Electrochim. Acta* **2019**, *304*, 360–369. [[CrossRef](#)]
42. Zhang, S.; Su, W.; Wei, Y.; Liu, J.; Li, K. Mesoporous MnO₂ structured by ultrathin nanosheet as electrocatalyst for oxygen reduction reaction in air-cathode microbial fuel cell. *J. Power Sources* **2018**, *401*, 158–164. [[CrossRef](#)]
43. Yang, W.; Chata, G.; Zhang, Y.; Peng, Y.; Lu, J.E.; Wang, N.; Mercado, R.; Li, J.; Chen, S. Graphene oxide-supported zinc cobalt oxides as effective cathode catalysts for microbial fuel cell: High catalytic activity and inhibition of biofilm formation. *Nano Energy* **2019**, *57*, 811–819. [[CrossRef](#)]

44. Divya Priya, A.; Deva, S.; Shalini, P.; Pydi Setty, Y. Antimony-tin based intermetallics supported on reduced graphene oxide as anode and MnO₂@rGO as cathode electrode for the study of microbial fuel cell performance. *Renew. Energy* **2020**, *150*, 156–166. [[CrossRef](#)]
45. Yan, Y.; Hou, Y.; Yu, Z.; Tu, L.; Qin, S.; Lan, D.; Chen, S.; Sun, J.; Wang, S. B-doped graphene quantum dots implanted into bimetallic organic framework as a highly active and robust cathodic catalyst in the microbial fuel cell. *Chemosphere* **2022**, *286*, 131908. [[CrossRef](#)] [[PubMed](#)]
46. Nancharaiah, Y.V.; Venkata Mohan, S.; Lens, P.N.L. Metals removal and recovery in bioelectrochemical systems: A review. *Bioresour. Technol.* **2015**, *195*, 102–114. [[CrossRef](#)] [[PubMed](#)]
47. Narasingarao, P.; Häggblom, M.M. Identification of anaerobic selenate-respiring bacteria from aquatic sediments. *Appl. Environ. Microbiol.* **2007**, *73*, 3519–3527. [[CrossRef](#)] [[PubMed](#)]
48. Rege, M.A.; Yonge, D.R.; Mendoza, D.P.; Petersen, J.N.; Bereded-Samuel, Y.; Johnstone, D.L.; Apel, W.A.; Barnes, J.M. Selenium reduction by a denitrifying consortium. *Biotechnol. Bioeng.* **1999**, *62*, 479–484. [[CrossRef](#)]
49. Samsudeen, N.; Sharma, A.; Radhakrishnan, T.K.; Matheswaran, M. Performance investigation of multi-chamber microbial fuel cell: An alternative approach for scale up system. *J. Renew. Sustain. Energy* **2015**, *7*, 043101. [[CrossRef](#)]

Disclaimer/Publisher’s Note: The statements, opinions and data contained in all publications are solely those of the individual author(s) and contributor(s) and not of MDPI and/or the editor(s). MDPI and/or the editor(s) disclaim responsibility for any injury to people or property resulting from any ideas, methods, instructions or products referred to in the content.